

## FIELD SURVEY OF *DRACAENA CINNABARI* POPULATIONS IN FIRMIHIN, SOCOTRA ISLAND: METHODOLOGY AND PRELIMINARY RESULTS

RADIM ADOLT<sup>1</sup>, PETR MADĚRA<sup>2</sup>, JOSEF ABRAHAM, PETR ČUPA<sup>3</sup>,  
MARTIN SVÁTEK<sup>2</sup>, RADIM MATULA<sup>2</sup>, JAN ŠEBESTA<sup>2</sup>, MARTIN ČERMÁK<sup>2</sup>,  
DANIEL VOLAŘÍK<sup>2</sup>, TOMÁŠ KOUTECKÝ<sup>2</sup>, MARTIN REJŽEK<sup>2</sup>, MARTIN ŠENFELDR<sup>2</sup>,  
JIŘÍ VESKA<sup>2</sup>, HANA HABROVÁ<sup>2</sup>, ZDENĚK ČERMÁK<sup>2</sup>, PETR NĚMEC<sup>2</sup>

<sup>1</sup>*Forest Management Institute Brandýs nad Labem, NFI Methodology and Analysis, Náměstí Míru 497,767 01 Kroměříž, Czech Republic, email: adolt.radim@uhul.*

<sup>2</sup>*Faculty of Forestry and Wood Technology, Mendel University in Brno, Zemědělská 3, 613 00 Brno, Czech Republic, email: xcupa@mendelu.cz, xmadera@mendelu.cz*

<sup>3</sup>*Lower Morava Biosphere Reserve, Lednice*

**Received:** 7<sup>th</sup> March 2014, **Accepted:** 10<sup>th</sup> April 2014

### ABSTRACT

Between 2010 and 2011 a field survey dedicated to *Dracaena cinnabari* (DC) population was conducted in Firmihin, Socotra Island (Yemen). It's main goal was to collect data that would make it possible to unbiasedly estimate main characteristics of the local DC population. Our motivation was to provide reliable information to support decision-making processes as well as other research activities. At the same time we were not aware of a survey which could provide this kind of statistical-sound estimates for the whole population covering an area of almost 700 ha.

This article describes how the survey has been planned and carried out in practice. In addition, we also provide a set of preliminary estimates of the main DC population figures - totals and per hectare densities of stems, overall and partitioned according to predicted crown age. Among estimated parameters there are also mean crown age and proportions of predefined age classes on the total number of living DC stems. These estimates provide an explicit information on age structure of the whole DC population in Firmihin.

Although we collected data on more than one hundred randomly located plots, the reported accuracy of our estimates is still rather limiting. We discuss several possibilities to obtain more accurate results or at least to approach the supposedly lower true variance that can't be calculated by approximate techniques applied here.

The design and concept of our survey makes it possible to evaluate changes over time on stem by stem bases and to generalize these stem-level details to the whole population. Mortality, regeneration and even change of population's mean crown age can be estimated from a future repeated survey, which would be extremely useful to draw firm conclusions about the dynamic of the whole DC population in Firmihin.

## INTRODUCTION

*Dracaena cinnabari* (further abbreviated as DC) is one of the key endemic species of Socotra Island (Miller et al., 2004). It is a dominant flagship tree shaping the landscape character of Socotra (De Sanctis et al., 2013). DC woodlands, according to Mies & Beyhl (1996) remnants of the Mio-Pliocene Laurasian subtropical forests, contribute to the high biodiversity and belong to the most important and peculiar plant communities of the island (Brown & Mies, 2012).

In the past, this unique ecosystem was present over large areas of the former Tethys, but in the Pliocene it was disrupted by climate change causing the desertification of North Africa (Axelrod, 1975). Today, together with another *Dracaena* tree species, DC represents a well-known example of the biogeographic disjunction between East and West Africa (Adolt & Pavliš, 2004; De Sanctis et al., 2013).

The genus *Dracaena* is exceptional among monocotyledonous plants because of its ability of secondary thickening of stems and roots (Razdorskij, 1954; Zimmermann & Tomlinson, 1969). Most of *Dracaena* species grow as shrubs or geophytes. Only six species (*D. cinnabari*, *D. serrulata*, *D. ombet*, *D. schizantha*, *D. draco* and *D. tamaranae*) have the growth habit of a tree typically occurring in thermo-sclerophyllous plant communities of tropical and subtropical regions (Marrero et al., 1998).

The most extensive population of any arborescent *Dracaena* sp. on Earth is the DC forest found in Firmihin. It is one of the most interesting localities on Socotra and, at the same time, one of the oldest forest ecosystems worldwide (Miller & Cope, 1996). On Socotra Island, DC occurs in altitudes from 323 to 1483 m a.s.l., with a mean annual temperature of 19.8–28.6 °C and an annual precipitation of 207–569 mm (Kurschner et al., 2006; Attorre et al., 2007).

The best contemporary distribution of DC forests and woodlands was published by (Král, Pavliš, 2006), who estimated the total area of habitats with presence of DC to 7230 ha (6200 ha of DC woodlands, 230 ha of DC forests and 800 ha of mountain forests with DC admixture).

In the past, DC forests were presumably present over larger areas of the island (Habrová, 2004; Attorre et al., 2007). Remnants of these unique woodlands are found in Firmihin, Momi, Haggeher Mts. and Dixam. Several smaller and disrupted populations exist on Kilim, Sirahan, Shibhon and other possibly less known localities. According to Attorre et al. (2007) DC occupies only 5% of its current potential habitat. Conditionally on a specific climate change scenario leading to increased aridity, the authors concluded that the current potential habitat of DC would be reduced by 45% in 2080. Only two out of the nine remnant areas should be considered as potential refugia (Attorre et al., 2007).

Despite of long-term adaptations of DC trees to climate conditions, present tree populations do have evidently unbalanced age structure with prevailing disorganization of woodland structure and lack of natural regeneration (Habrová et al., 2009). This species is endangered by overmaturity and fragmentation of population in most areas (Van Damme & Banfield, 2011). Hence, DC populations are getting older and step by step disappearing.

Two hypotheses have been recently proposed to explain recession of DC community. The first one fully blame animal grazing as the main driving force of unsatisfactory tree regeneration and prevailing absence of younger age classes (Adolt & Pavliš, 2004). The second one considers global climate change as the main factor (Miller & Morris, 2000). No matter the reason, DC forests and woodlands belong to threatened communities today (Scholte & Degeest, 2010; Scholte et al., 2011).

Hubálková (2011) and Habrová et al. (2009) published prediction models of future development at selected localities, based on detailed description of stand structure

(Habrová & Maděra, 2004) and the original methodology of DC crown age estimation by Adolt & Pavliš (2004). For the period of next 100 years the authors predicted a decrease of DC abundance by 36% (Hubálková, 2011) or 37% respectively (Habrová et al., 2009).

Adolt et al. (2012) published an improved methodology of DC crown age estimation which might be very useful because the knowledge of age structure is essential to draw statistical-sound inference about this unique ecosystem. However, it is not only the statistical model to predict crown age what is needed to achieve our goals of providing reliable figures about the largest DC population found on Socotra.

Firmihin plateau covers an area of almost 700 ha. Not surprisingly, most environmental parameters vary significantly over the whole region and also the structure of DC population is fairly heterogeneous in terms of its density, dimensions and age of specimens. The extent of Firmihin plateau together with an elevated number of DC stems are the two decisive factors suggesting that the population-level inference must be based upon some sort of sampling.

To the best of our knowledge, before the survey presented here was launched, no statistical-sound, design-unbiased information on the total number of stems, their spatial density, age structure nor any other parameters of any DC population on Socotra was published. Of course, there were many sample plots established and measured by several teams and conclusions were drawn based on the data obtained. But let's try to answer following questions! What was the sampling design used? How were the positions of these plots chosen? What are the populations these plots should represent? Do these populations have a clear definition? How is the representativeness of survey data achieved? What is the accuracy of estimates? Are we able to derive reliable confidence intervals for all parameters estimated? Any difficulties in answering of these questions would indicate that sampling issues were not taken into account appropriately.

The idea of sampling as an alternative to full enumeration (census) has been introduced long time ago. Laplace (1783) was presumably the first scientist who applied and also published principles of sampling. He paid considerable attention to uncertainty of estimates and derived minimum sample size to achieve required accuracy of an estimator for the population of France.

At the end of 19<sup>th</sup> century, Norwegian statistician A. N. Kiaer proposed the usage of representative sampling (Bellhouse, 1988). It was Kiaer who contributed to the general acceptance of this concept. Until the famous paper of Neyman (1934), representativeness of samples used to be achieved by purposive selection. Using this approach researchers judge themselves what population elements are representative and therefore eligible for sampling. Neyman (1934) presented reasons why randomization should be preferred to purposive sampling. He also provided firm statistical framework to capture uncertainty via confidence intervals for sample estimates, which are based on their distribution among all possible samples of given size (design-based approach to uncertainty assessment).

Although randomization of sampling was first introduced by Bowley in 1912, it was the work of Neyman (1934), which led to its general acceptance among statisticians (Bellhouse, 1988). The early principles evolved to the current theory of probability sampling (Cochran, 1977). During 1950's, modern sampling theory was already well established and generally accepted.

In the second half of 20<sup>th</sup> century an alternative concept of uncertainty - the model-based or model-dependent approach was introduced by Godambe (1955) and further developed by Cassel et al. (1977). Under this framework, a correct assessment of uncertainty of an estimator relies on assumptions about the stochastic process that generated the population. These assumptions are expressed by a model formulation. Careful validation of the

constructed model is indispensable, but of course, time consuming as well. Moreover, not only the analyst, but also the end-user should be convinced that the model applied to survey data is plausible. For small sample sizes and under reasonable model performance, the model-dependent approach can lead to more accurate estimates than strictly design-based alternatives (Rao, 2003; Mandallaz, 2007).

The application of sampling methods has a long tradition in forestry. In 1830, Israel af Ström conducted a small-scale forest inventory in Sweden using the early principles of sampling (Kangas et al., 2006). First national forest inventories, which involved sampling mechanism, were launched in Scandinavia (Norway, Sweden, Finland) around 1920.

The survey presented here is based on a contemporary concept being in use by most national forest inventories. The methodology is strictly design-based, so only minimal assumptions about the population itself are necessary. In fact, the large sample convergence of estimators to normality is the only theoretical precondition (section 2.8).

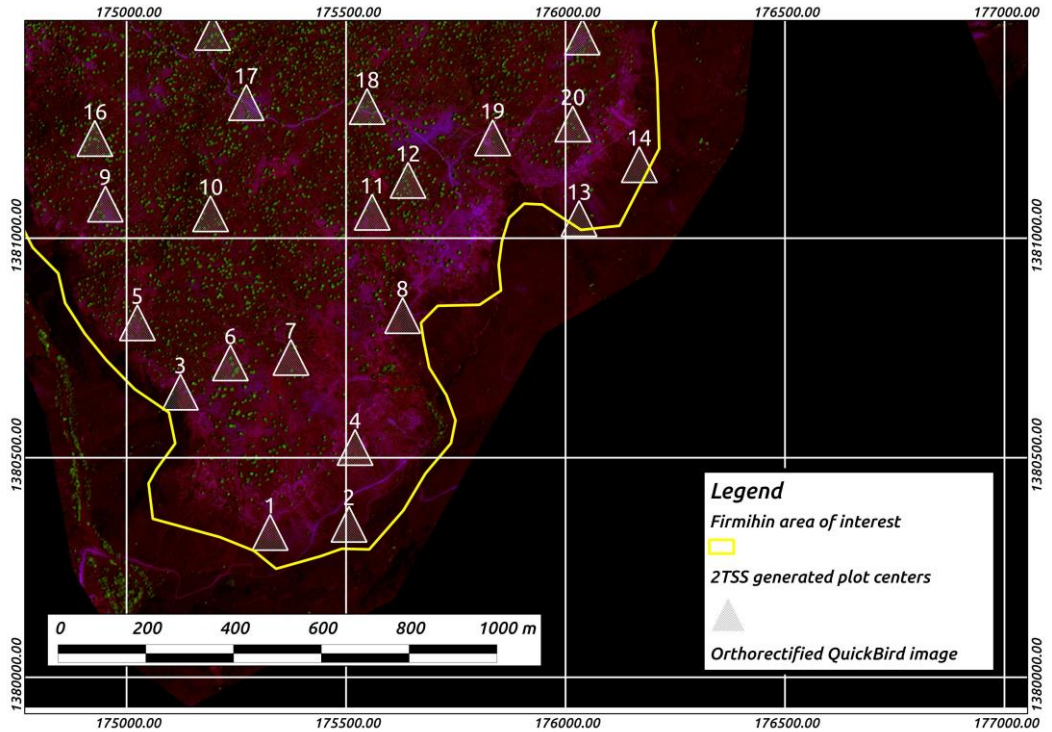
During the survey, only nondestructive measurement methods were applied. No animals nor plants were killed or harmed in the course of fieldworks. We worked with the hope, wish and belief that results of this survey will contribute to the preservation of Socotra's unique nature and consequently bring an indirect benefit to local people.

## **DATA COLLECTION AND PROCESSING**

### **Definition of the AOI**

One of the very first and fundamental steps to do was the definition of an area of interest (AOI). All DC specimens within this area are considered members of the target population. This task has been accomplished by means of visual vectorization of Firmihin's perimeter using orthorectified QuickBird imagery. Border line was drawn along edges of the Firmihin plateau, which could be visually perceived as a transition between accessible, predominantly flat terrain and adjacent steep slopes of two giant wadis - Darho and Ezgeko. The borderline joins these two wadis in northern part of Firmihin, where it runs across a saddle connecting Firmihin plateau to Diksam highlands. Figure 1 depicts southern part of the Firmihin AOI, the total area of which amounts to 687.20 ha. Quite inevitably, some parts of the AOI are in fact not accessible, which has been registered during field works.

**Fig. 1: Southern part of the Firmihin area.** The (yellow) borderline was delineated using orthorectified QuickBird imagery. Triangles depict positions of plots, as they were generated according to the 2TS design.



### Spatial distribution and density of sample plots

The way how sample locations are distributed within a survey area influences the precision of estimators. Natural populations use to exhibit some degree of spatial correlation - i.e. elements close together tend to be more similar than those separated by larger distances (Matern, 1960; Stevens, 1997). A regular pattern of sample locations typically, but not necessarily, leads to higher within-sample variability whereas variability among all possible samples decreases. From sample to sample the estimates tend to change less than if sample locations were chosen completely at random (Uniform Random Sampling further abbreviated as URS) (Quenouille, 1949; Matérn, 1960; Cordy & Thompson, 1995; Stevens, 1997; Ripley, 2004).

There are many different sampling techniques, which generate a regularized coverage of a survey area by sample locations. The best known are systematic and spatially stratified designs. Both have several variants, see Quenouille (1949) or Cochran (1977, section 8.13) for an overview. Spatially stratified designs are always at least as precise as the URS (Haber, 1966, 1967; Barabesi & Franceschi, 2010). However, this statement does not hold for systematic designs (centric or aligned), which might be less precise than URS provided spatial periodicity of population values exists (Cochran, 1977; section 8.8, Ripley, 2004; section 3.2).

For our survey we chose random origin, spatially stratified sampling with a regular tessellation of the survey area by congruent squares. This design is known as Two step

Tessellation Stratified (2TS) (Cordy & Thompson, 1995). In the first step a survey area is tessellated by randomly shifted regular grid (squared cells). The second step corresponds to completely random generation of one inventory point in each cell. Positions of inventory points are generated independently between any two cells of the whole grid. To clarify the approach let's describe the generation of inventory points by 2TS in more detail. For simplicity of explanation we left out details related to the generation of a sequence of sampling sub-grids with decreasing density of inventory points.

Typically irregularly shaped inventory regions and their arbitrary partitions (areas of interest, geographical domains) can't be tessellated by an integer number of congruent inventory blocks. Therefore, 2TS algorithm is implemented using an adjusted bounding box of the inventory region (actually the whole Socotra Island). At first, the position of the original bounding box is shifted in the  $(x; y)$  plane (UTM coordinate system, Zone 40N) in south-west direction. The absolute values of the components  $(-\Delta x; -\Delta y)$  of the shift correspond to the size of the predefined inventory block (rectangle or square for simplicity) in the respective direction. From the south-western tip of the shifted bounding box (the grid origin) new eastern and northern limits are calculated in a manner that guaranties that the whole inventory region (union of all potential areas of interest) is fully covered by the resulting rectangle of minimum possible size and that the rectangle itself can be partitioned into an integer number of predefined inventory blocks. In the next step the rectangle's origin is translated again, this time in north-east direction, by a random vector with components  $(+\Delta x; +\Delta y)$  generated independently in the interval between zero and the block size in the respective direction (two independent samples from a uniform probability distribution). Finally a random position of a single inventory point is generated within each of the inventory blocks, that congruently tessellate the resulting rectangle - the support covering the whole inventory region.

In many practical situations 2TS design is significantly more accurate than the URS. However, under somewhat peculiar circumstances of nearly constant value of local density the accuracy of URS may outperform 2TS (Barabesi & Franceschi, 2010; section 2.2). Fortunately this situation doesn't occur in most environmental surveys. Our  $D$  (Firmihin AOI) is irregularly shaped, but local densities corresponding to our target parameters are far from being constant over  $D$ . Therefore, we are quite sure, 2TS design is definitely a better choice for our survey than the URS alternative. Barabesi & Franceschi (2010) proved large sample convergence of 2TS total estimator to normality. This property is necessary to construct confidence intervals based on the assumption that the distribution of an estimator is normal.

**Table 1: Survey metadata**

Parameter	Value
Extent of Firmihin survey area [ha]	687.20
Total number of plots located in Firmihin survey area	107
Number of plots with accessible plot center	101
Number of plots with alive DC stems ( $h > 1.3$ .m) registered	98
Area of circular segment with 25 m radius [ha]	0.1964
Area of circular segment with 15 m radius [ha]	0.0707
Number of alive DC stems ( $h > 1.3$ m), circular segments, 25 m radius	1930
Number of alive DC stems ( $h > 1.3$ m), circular segments, 15 m radius	727

Generation of sample locations has been implemented using digital map of the whole Socotra Island, hence the resulting locations might serve to a future Island-wide survey(s). The grid is formed by squares 250 m×250 m - each containing one randomly located inventory point. Sub-grids of decreasing spatial resolution (reductions of sampling density by factor of 4, 16, 64 and so on) were defined by restricted random sub-sampling. These may be used for less intensive sampling of larger areas or for more detailed surveys, which would not be feasible on the big number of plots corresponding to the full sampling grid resolution. In total 107 inventory points (full resolution, 250 m) were generated within the Firmihin AOI. This number would obviously fluctuate if we repeatedly generated the same type of sampling grid without changing the shape and size of inventory blocks. All inventory points (plots) located in Firmihin AOI were surveyed during our field campaign.

### Sampling protocols at the plot level

Population of DC stems in Firmihin have been partitioned into three major subpopulations - living stems, death stems and regeneration. Living stems with measurable diameter in breast height (dbh, height  $\geq 1.3$  m) were further structured according to the number of leaf rosettes. For each subpopulation, specific sampling protocols were used, see table 2 for an overview.

For the purpose of this survey, we strictly distinguish between stems and trees. The term stem does not refer to a tree organ in common (biological) sense (an organ located between root system and crown). A tree may be composed by one or several stems - subjects of our dendrometric measurements and mapping. In most circumstances there is no difference between stem and tree because both terms refer to the same object including all plant organs (roots, stem in the biological sense, crown, branches, leaves etc.). However, if the tree axes is branched above ground but still below breast height, the tree is composed by several stems which correspond to individual offshoots distinguishable at breast height (dbh measurable). The definition of sampling protocols as well as all dendrometric measurements is straightforward for stems, but not for trees in the general case. The above described peculiarity should be taken into account when results of this survey are interpreted, yet the proportion of DC trees composed by two or more stems is fairly negligible in Firmihin.

Next step was to decide, how particular populations will be selected i.e. to define sampling protocols. Circular sample plots represent a natural choice in case of living stems. Using circular plots the decision, whether particular stem has been selected or not, is based on a simple measurement of distance between the plot center and the stem axes at breast height (1.3 m).

**Table 2: Subpopulations of *D. cinnabari* surveyed in Firmihin**

	subpopulation	Sampling device
<b>living stems</b> (dbh measurable)	less than 6 leaf rosettes at least 6 but less than 15 leaf rosettes 15 or more leaf rosettes	circle with $r = 25$ m (additional variables surveyed on living trees in a circle with $r = 15$ m)
<b>death stems</b>	standing, preserved crown stem residues and stumps	
<b>regeneration</b> (dbh not measurable)	height $< 25$ cm $25 \text{ cm} \leq \text{height} < 50$ cm height $\geq 50$ cm	circle with $r = 1$ m circle with $r = 3$ m circle with $r = 5$ m

Sampling living stems with a measurable dbh (minimum height of 1.3 m) was conducted by two concentric circular segments centered at the main inventory point. The circle sizes were derived as follows. First, single stems were digitized using orthorectified QuickBird imagery on circular plots of an ad-hoc size (radius 12.62 m, area 500 m<sup>2</sup>) centered at 107 generated inventory points (section 2.2). This way, we could at least roughly estimate the average number of stems per plot of given size and obtain some reference what time and how many surveyors are needed to finish measurements on one single plot with arbitrary radius. The radius  $r = 25$  m of the larger circle was deduced from the requirement to have on average 12 - 16 stems registered on each sample plot and from the visually estimated density of stems per unit area. This circle size was considered still within the range of straight visibility in Firmihin. In an ideal case, stem positions are targeted using one distance-angle measurement only. This is possible only if there are no obstacles between the surveyor's position (most typically at plot center) and the stem (reflector's position). In all other circumstances the surveyor has to adjust his position by establishing one or several reference points, which costs additional time.

The average number of 12-16 stems per plot was subjectively agreed to be a reasonable compromise between, what time is needed to reach and establish the plot, what time is consumed for its complete measurement and what is the information gain. Let us recall also the fact that the more sample locations (plots), the larger portion of the overall variability is captured within the whole sample and the more accurate will be our estimates (Mandallaz, 2007; chapter 9). Consequently, we should prefer a higher number of bigger plots over a lower number of smaller plots because the extra measurements on larger plots tend to capture more or less the same local information.

**Table 3: Variables assessed on subpopulations of *D. cinnabari* in Firmihin**

subpopulation	sampling device	variable
<b>living stems</b> (dbh measurable, variables assessed on individual stems)	circle with $r = 25$ m	stem position subpopulation of living trees presence/absence of flowers presence/absence of fruits dbh [mm]
	circle with $r = 15$ m	total height [m] crown base height [m] total number of leaf rosettes number of leaf rosettes with fruit ponicles number of leaf rosettes with inflorescences mean number of branching orders
<b>death stems</b> (variables assessed on individual stems)	circle with $r = 25$ m	stem (stump) position subpopultaion of death stems
	circle with $r = 15$ m	mean number of branching orders (standing death stems, preserved crown)
<b>regeneration</b> (dbh not measurable, counts per circle)	circle with $r = 1$ m	no. of specimens, height < 25 cm
	circle with $r = 3$ m	no. of specimens, 25 cm ≤ height < 50 cm
	circle with $r = 5$ m	no. of specimens, height ≥ 50 cm

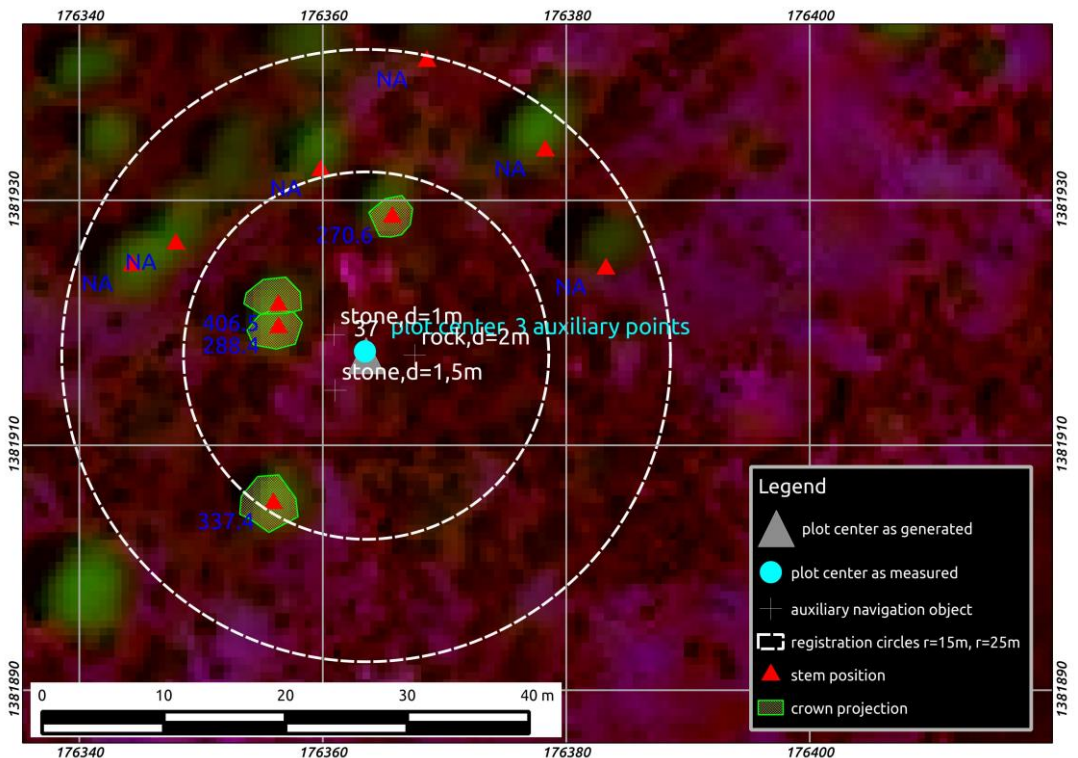
Relatively wider scope of the survey resulted in a larger amount of attributes to be assessed on sample stems. Therefore, we established a smaller circle with radius of 15 m, where a set of time consuming variables has been assessed. In table 3 there is an overview of attributes assessed on living stems according to the their position relative to the two concentric circles. Figure 2 shows the situation on one of the sample plots.



Compared to living and mature stems, death trees and regeneration specimens are relatively rare in Firmihin. Survey of these subpopulations could be carried out by distance sampling - registering specimens detected on both sides of a transect and measuring their distance perpendicular to the transect line, see (see Buckland et al., 1993). This sampling technique should be ideally carried out by one team to avoid effects of particular surveyors on detection probabilities. Many of our surveyors were under-graduated students without any previous exposition to field surveys of this kind and with almost no experience with Field-Map technology. Therefore, a careful training was indispensable. In addition, there were more teams needed to finish field works in time. Because distance sampling was considered rather demanding under these circumstances, we finally decided to sample death stems by a larger circular segment with radius of 25 m and center coincident with the 2TS inventory point (section 2.2).

Regeneration was sampled using a tract of four inventory plots located 10 m apart from the 2TS inventory point in north, south, east and west direction. There were three concentric circular segments established on each plot of the tract. These were used to register the number of regeneration specimens in each particular subpopulation, see table 2 for details. Using a tract of four plots increases a chance of selecting at least some regeneration individuals.

**Fig. 2: Survey situation on plot nr. 37.** Blue labels near stem positions show stem dbh [mm].



### Equipment

Survey data were collected digitally right in the field using a rugged tablet Getac E100, with an integrated GPS instrument and Field-Map software (manufactured by IFER Ltd). The tablet was mounted on Manfrotto monopod.

Approximately one fourth of plots (first plots according to the plot numbers) were surveyed using MapStar (electronic angle-decoder) and ForestPro (range finder, clinometer, hypsometer). These instruments (both by Laser Technology Inc.) were used for navigation to inventory points, mapping of auxiliary navigation objects and DC stems. TruePulse (angle-encoder, clinometer and hypsometer by Laser Technology Inc.) was used for tree height measurements on this first batch of plots. On the remaining majority of plots TruePulse was used as a replacement for MapStar and ForestPro, because the later suffered from elevated humidity (rain, mist). Moreover, the set with MapStar and ForestPro was found unreasonably heavier by most surveyors. Tree heights were measured by Silva-ClinoMaster on these plots. Figure 3 shows the field equipment with MapStar and ForestPro instruments.

Diameters in breast height (dbh) were measured either by metallic tape (southern part of Firmihin AOI, where larger trees were found) or by electronic caliper manufactured by Haglöf Sweden AB.

Positions of inventory points (plot centers) were fixed by geodetic landmarks (plastic-coated metallic harpoons).

**Fig. 3: Survey group leader Sir Joseph Abraham holding a Field-Map set.** The device is composed by rugged tablet (Getac E100), MapStar (digital angle encoder), ForestPro (clinometer, height meter, range finder) and an external battery. All pieces mounted on a Manfrotto monopod.



### Field survey organization and workflow

Three missions to Socotra were organized. The first one in May-June 2010, the second in October 2010 and the last one in January 2011. More than thirty people contributed to field works. Table 1 shows survey metadata.

Since there was only one full equipment and because the field works were quite

demanding, we organized one to three (most typically two) work-ships a day. Each work-ship was ensured by a different survey group. Typically there were four to six surveyors in each group, depending on organizational circumstances. The group leader was responsible for mapping of objects and data registration in Field-Map software as well as the overall coordination of field works. Two people used to cooperate directly with the group leader - they were moving around the plot with poles and reflectors in order to map various kinds of objects (position on auxiliary navigation objects, position of stems, establishing the tract for regeneration survey, mapping of crown projections of DC stems). Remaining surveyors conducted an assessment of DC stems and regeneration.

The survey on each particular plot always started by navigation to given 2TS inventory point (section 2.2). This has been facilitated by the Getac's internal GPS, which was linked to Field-Map software showing the remaining distance and bearing. In Field-Map we used compositions of an orthorectified QickBird mosaic with several SHP layers - Firmihin AOI, generated plot centers (2TS inventory points), plot centers as measured and auxiliary navigation points, see figure 2.

First stage of navigation looked-like free walking to the proximity of the 2TS inventory point. At a distance no greater than 15-30 m (one straight distance measurement) the group leader stabilized its position in the digital map by at least two hundred GPS measurements. Next a sequential navigation started. The leader instructed one of the surveyors carrying a pole with a reflector how far and in which direction he should go to reach the generated plot center. This has been done repeatedly until the desired position was reached with cm-accuracy. In case of visibility problems, the group leader moved to the last position of the surveyor and translated his position in the map. The final surveyor's position was accepted in Field-Map as the actual position of the equipment and a corresponding point was introduced into SHP layer (plot centers as measured).

**Fig. 4: Plot center stabilization.** Positions of all surveyed plot centers were stabilized by geodetic landmarks. In addition three auxiliary navigation objects were identified, mapped and photographed.



Positions of plot centers were fixed by geodetic landmark (metallic, plastic-coated pole). In case the landmark could not be hammered right at the plot center, it has been shifted to

a nearest suitable location (the landmark, not the whole plot). The final landmark position has been introduced to SHP layer (plot centers as measured) with an indication that the landmark - not the 2TS inventory point nor the plot center, has been shifted. There were several reasons, why geodetic landmark sometimes could not be fixed right at the plot center. Most typically the plot center was located on a rock or a big boulder or it was not accessible. Geodetic landmarks were shifted also in cases, when the plot center was on a location where long-term stabilization was unlikely e.g. on or in a proximity of a road, in a stream, on locations affected by heavy soil erosion etc.

Plots corresponding to 2TS inventory points located within Firmihin AOI were stabilized only if some part of any circular segment was accessible. In other cases no stabilization was done because no measurements could be taken on such plots. Full survey was conducted on accessible parts of all stabilized plots. Using this approach, no edge-effect compensation due to inaccessibility is needed. Nevertheless, compensation of edge-effect due to proximity of population elements to AOI border was neglected in our analysis. Therefore, some (negligible) underestimation of totals is present in our results. The principle of edge-effect along with various compensation methods is nicely captured by Gregoire & Valentine (2008, section 7.5).

Three auxiliary navigation objects were identified in the proximity of each landmark. These were mapped into a SHP layer, described by attributes (what type of object, what size, specific features) and photographed, see figure 4. A detailed picture of the plot center with its surroundings was taken too. This documentation is essential for a future survey on identical locations because it will be necessary to assess changes on stem by stem bases. Unfortunately this activity was sometimes done unsatisfactorily by unexperienced surveyors as was recognized during the post-processing of photographs. Luckily we concluded that for most plots we have at least three useful photographs (landmark's position is always one of them) and for very few plots we have just two.

In the next stage, positions of the north, south, east and west regeneration plot were established in the field. Registration and mapping of stems on the main plot was done respecting thresholds given in table 2.

Further measurements followed as described in the first paragraph of this section. All data were stored in Field-Map software, which used predefined scripts to check data consistency and to adjust the graphic user interface (showing and hiding dialogs in response to currently entered data).

Mapping of objects was typically conducted from the position of the landmark, although there were situations when reference points had to be established (limited visibility). All navigation and mapping tasks were done in UTM coordinate system using zone 40N.

### **Digital data processing**

Data collection and mapping was done using the Field-Map technology (IFER Ltd.). All survey data have been saved in a digital format right in the moment of acquisition. Field-Map uses Microsoft Access database for numeric attributes and SHP files for spatial data storage. Spatial as well as attribute data were migrated into PostgreSQL 9.1 database (<http://www.postgresql.org/postgresql.org>) with PostGIS 2.0 spatial extension (<http://postgis.net/postgis.net>). Calculation of results was based on a set of our own functions written in PL/R procedural language (<http://www.joeconway.com/plrjoeconway.com>) under PostgreSQL. These functions use a self-coded R library called estimators4nfi, which was implemented in S4 classes (R Core Team, 2013). This library has been developed for the purposes of Czech national forest inventory (<http://www.uhul.cz/>).

### Parameter estimation

Estimation of target parameters was based on continuous population approach to forest inventory proposed by Mandallaz (1991, 2007). The author introduced a function called local density, which translates the problem of estimation by circular plots (sampling a finite population of stems) to point sampling from a continuum (an infinite population of points). Estimations of any stem-related quantity as well as estimations of the total area of accessible land could be based on a common theory - an extension of the Horwitz-Thompson theorem to point sampling from a continuous universe, further abbreviated as HTC (Cordy, 1993).

Sections 2.7.2 and 2.7.3 present estimators that can be derived from HTC specifically for Uniform Random Sampling (URS). Under the URS design a fixed number  $n_D$  of inventory points is selected from the area of interest - the geographical domain  $D$  (Firmihin AOI). Let us emphasize the term *fixed number of inventory points*, which means that the sample size  $n_D$  is constant among (hypothetical or real) replications of the sampling process (repeated generations of sample locations according to the same sampling design). Attentive readers already noticed that our sample locations (inventory points) were generated by 2TS design - not the URS (section 2.2). In our analysis, URS theory was used only as an approximation for the purpose of variance estimation.

From the detailed description of the 2TS algorithm in section 2.2 it is evident that over any set of replicated 2TS samples the number of inventory points located in  $D$  (the inventory region itself or its arbitrary subset - here the Firmihin AOI) varies from sample to sample due to random shifts of the support relative to  $D$  and also as a consequence of random positioning of inventory points within inventory blocks that were not entirely located within  $D$ . The expected sample size is defined by

$$\bar{n}_D = \frac{\lambda(D)}{\lambda(c)}, \quad (1)$$

where  $\lambda(D)$  is the area of  $D$  and  $\lambda(c)$  is the area of a single inventory block.

HTC leads to identical estimators of total for URS as well as 2TS design, provided the later is defined as unbiased conditionally on the actual number of inventory points in  $D$  (see Cordy, 1993; pages 361). Estimators unbiased conditionally on particular sample size  $n_D$  have the property

$$\mathbb{E}[\hat{\theta} | n_D, n_D \geq 1] = \theta, \quad (2)$$

where  $\theta$  is the true value of the population parameter in  $D$  (Firmihin AOI).

Based on HTC theorem variance of the total estimator as well as its design-unbiased estimators can be derived specifically for 2TS design (Stevens, 1997). Stevens (1997) and Stevens & Olsen (2003, 2004) indicated that these variance estimators were often unstable (they themselves have rather higher variance), which has been confirmed by several other authors (Cordy & Thompson, 1995; Cooper, 2006).

Cordy & Thompson (1995) designed an approximate variance estimator, which performed best among other candidates evaluated by means of simulated sampling from a range of artificial populations. It was found to be stable and almost unbiased. Stevens & Olsen (2003) proposed another approximately unbiased and stable variance estimator. So far, we have not

implemented any of these promising variance estimators for 2TS and its GRTS generalization. For this study we used URS approximations only (sections 2.7.2 and 2.7.3).

Under positive spatial correlation of local density, and if the local density itself (section 2.7.1) does not exhibit any periodic pattern, the URS variance estimator applied to systematic or spatially stratified sampling is positively biased (conservative) (Matérn, 1960; Cordy & Thompson, 1995; Heikkinen, 2006). Conservativeness of an estimator of variance is expressed by

$$\mathbb{E}[\widehat{\mathbb{V}}_{URS}(\hat{Y}_{n_D}|n_D, n_D \geq 2)] > \mathbb{V}_{2TS}(\hat{Y}_{n_D}|n_D, n_D \geq 2). \quad (3)$$

Conservative variance estimators usually lead to conservative confidence intervals (section 2.8).

In analogy to totals, properties of variance estimators and confidence intervals can be also conditioned on realized sample size. As we used the conditional approach for variance estimation, the expected properties of our confidence intervals can be interpreted conditionally on realized sample size (Särndal et al. 2003; section 7.10).

#### A. Local density

A crucial property of local density function  $Y(x)$  depicts an equation

$$\int_D Y(x)dx = Y, \quad (4)$$

which says, that for given variable the sum of local density over the entire estimation domain  $D$  (the area of interest) equals the true total  $Y$  in  $D$ .

Furthermore, the expected value of local density equals the mean value of given variable in  $D$

$$\mathbb{E}[Y(x)] = \frac{1}{\lambda(D)} \int_D Y(x)dx = \bar{Y}, \quad (5)$$

where  $\lambda(D)$  stands for the exactly known total area of  $D$ .

For the estimation of total land area belonging to a specific category  $K$  the local density on an inventory point  $x$  is defined as an indicator (dummy) variable

$$I_K(x) = \begin{cases} 1 & \text{IF } x \in K \\ 0 & \text{IF } x \notin K. \end{cases} \quad (6)$$

This definition was used to estimate the total area of accessible land within Firmihin AOI. For this purpose local density takes value of one on accessible inventory points and zero on inaccessible ones.

Estimators of stem-related quantities are based on the following definition of local density



$$Y_C(x) = \sum_{i \in \mathcal{P}} \frac{I_i(x) C_i Y_i}{\lambda(K_i)}, \quad (7)$$

where  $\lambda(K_i)$  is the area of inclusion zone  $K_i$  of stem  $i$ ,  $\mathcal{P}$  represents the set of stems located on accessible land within Firmihin AOI,  $I_i$  is an indicator (zero or one) variable taking value of 1 if and only if stem  $i$  is selected by corresponding circular segment established on the inventory point  $x$ ,  $C_i$  is an indicator variable taking value of 1 if and only if stem  $i$  belongs to particular subpopulation  $C$  (e.g. crown age class), term  $Y_i$  stands for the value of a variable observed on stem  $i$  for which the total or mean per unit area in  $D$  has to be estimated. In case of an estimation of total and stem densities per unit area,  $Y_i$  takes a constant value of 1. For an estimation of mean crown age,  $Y_i$  corresponds to crown age predicted for stem  $i$  (section 2.9).

The geometry of an inclusion zone  $K_i$  equals the geometry of sample plot (Gregoire & Valentine, 2008; section 7.4.1). More specifically, it corresponds to the circular segment by which the stem can be selected under given sampling protocol (see table 2 for an overview of sampling protocols). Stem  $i$  is selected if and only if any of the inventory points generated by the sampling design (2TS, see section 2.2) falls into its inclusion zone.

For this preliminary analysis we decided to use only stems located within the smaller circle ( $r = 15$  m), so we have effectively used  $\lambda(K_i) = \lambda(K) = 0.0707$  ha for all stems included in our calculations. The reasons were twofold. On one hand, we wanted to proceed quickly with data processing and publication and, on the other hand we preferred to keep the level of mathematical complexity on a reasonably simple level, convenient for a wider audience of readers.

Things would have become more complicated because our intention was to break down estimates of stem totals and per hectare densities according to predicted crown age classes. Moreover, from the user's perspective it is desirable that the sum of total as well as stem density estimates over all crown age classes exactly matches the figures for the (sub)population as a whole (additivity of estimators). For stems located inside the larger circle ( $r = 25$  m) we did not register the mean number of branching orders - a variable needed to predict crown age (section 2.9). Without an introduction of a more general concept of local density, the estimators per crown age class can only be based on a reduced set of stems located within the smaller circle ( $r = 15$  m). Nevertheless, for the whole (sub)population of living stems with a crown, there are two options how to estimate totals and stem densities per unit area. We could use either stems located in the smaller circles only (our actual choice leading to complementary figures between crown age classes and the whole) or all stems including those registered within the larger circles. Obviously, the later option brakes the desired additivity between the whole (sub)population and its partitions according to crown age classes.

### B. Estimation of totals and means

One-phase estimation total  $\hat{Y}_{n_D}$  (field data is the only source of information used) is given by

$$\hat{Y}_{n_D} = \begin{cases} \lambda(D) \sum_{x \in S, x \in D} \frac{Y(x)}{n_D} = \lambda(D) \hat{\bar{Y}} & \text{IF } n_D \geq 1 \\ 0 & \text{IF } n_D = 0, \end{cases} \quad (8)$$

where  $\lambda(D)$  is the exactly known area of  $D$  (Firmihin AOI) in ha,  $Y(x)$  is value of the corresponding local density at inventory (sample) point  $x$ ,  $n_D$  stands for the number of inventory points actually located in  $D$  (107 plots, conditional approach) and  $\hat{\bar{Y}}$  is the sample mean of local density over all inventory points in  $D$ . The sum iterates over all inventory points located in  $D$ .

An URS approximation of design-based variance of the  $\hat{Y}_{n_D}$  is given by

$$\hat{V}_{URS}(\hat{Y}_{n_D} | n_D, n_D \geq 2) = \frac{\lambda^2(D)}{n_D(n_D - 1)} \sum_{\substack{x \in S \\ x \in D}} [Y(x) - \hat{\bar{Y}}]^2. \quad (9)$$

Variance estimator of the mean  $\hat{\bar{Y}}$  is related to the variance estimator of the corresponding total  $\hat{Y}_{n_D}$  according to

$$\hat{V}_{URS}(\hat{\bar{Y}} | n_D, n_D \geq 2) = \lambda^{-2}(D) \hat{V}_{URS}(\hat{Y}_{n_D} | n_D, n_D \geq 2). \quad (10)$$

Both above variance estimators are expected to be conservative (no periodicity, positive spatial correlation, moderate sample size) conditionally on sample size i.e. condition (3) holds.

### C. Estimation of ratios

Several target parameters of our survey are defined as ratios of two unknown quantities. In theory, stem density can be defined as the ratio of total stem count and an exactly known surface area of  $D$  (Firmihin AOI). However, by field survey we can't estimate total stem count including stems on inaccessible land. Therefore, we cleverly redefine the total (and the population itself) including stems on accessible land only. Because total area of accessible land is not known it has to be estimated as well. Under these circumstances, it is reasonable to redefine stem density as a ratio of total stem count on accessible land and the unknown area of accessible land itself (see table 6).

Proportions of stems pertaining to predefined crown age classes were defined and estimated as a ratio of total number of stems falling to given crown age class to total number of stems. Both totals include only stems located on accessible land (see table 7).

Mean crown age is defined as a ratio of two unknowns - total crown age over all accessible stems and total number of stems with a crown, which are located on accessible land.



In general the estimator is either defined as a ratio of two total estimators or equivalently as a ratio of two means over  $D$ .

$$\hat{R}_{1,2} = \frac{\hat{Y}_{1,n_D}}{\hat{Y}_{2,n_D}} = \frac{\hat{\bar{Y}}_1}{\hat{\bar{Y}}_2} \quad (11)$$

Estimator  $\hat{R}_{1,2}$  is only asymptotically unbiased for  $R_{1,2}$ . Its bias decreases fairly quickly with sample size and it gets negligible already for moderate sample sizes (Cochran, 1977; section 2.11, Särndal et al., 2003; section 5.6).

An approximate variance estimator for  $\hat{R}_{1,2}$  according to (12) is based on Taylor linearization technique (Cochran, 1977; section 2.11; Särndal et al., 2003; section 5.6).

$$\hat{V}_{URS}(\hat{R}_{1,2} | n_D, n_D \geq 2) = \frac{\lambda^2(D)}{n_D(n_D - 1)\hat{Y}_{2,n_D}^2} \sum_{x \in D} Z_o^2(x) \quad (12)$$

The term  $Z_o(x)$  is a residual local density evaluated on inventory point  $x$  according to

$$Z_o(x) = Y_1(x) - \hat{R}_{1,2}Y_2(x), \quad (13)$$

where  $Y_1(x)$  and  $Y_2(x)$  represent local densities observed on the 2TS inventory point  $x$ . These two densities correspond to estimators in the nominator and denominator of  $\hat{R}_{1,2}$ .

Variance estimator (12) is expected to be less conservative than its analog (9) for totals, even though local densities corresponding to the nominator and denominator of  $\hat{R}_{1,2}$  show a substantial degree of spatial correlation. It is the residual variable  $Z_o(x)$  the distribution of which over  $D$  has the decisive influence on variance. Values of  $Z_o(x)$  are usually less spatially correlated than those of corresponding local densities. Therefore, a notable decrease of conservativeness is expected.

### Confidence intervals and the confidence level

Confidence intervals were constructed according to following equation

$$CI = \hat{\theta} \pm z_{(1-\alpha/2)} \sqrt{\hat{V}(\hat{\theta})}, \quad (14)$$

where  $\hat{\theta}$  is an estimator of an unknown value of a population parameter  $\theta$ ,  $\hat{V}(\hat{\theta})$  is an estimator of variance of  $\hat{\theta}$  and  $z_{(1-\alpha/2)}$  is the  $1 - \alpha/2$  quantile of standardized normal distribution. This approach approximates the true distribution of an estimator by normal probability distribution. Large sample convergence of 2TS total estimators to normality was proved by Barabesi & Franceschi (2010; see Result 2 in Appendix ). Of course the term *large sample* is somewhat arbitrary.

Confidence level of constructed intervals matches the probability  $P$  given by equation (15), where  $CI^-$  and  $CI^+$  are the lower and upper bounds.

$$P(CI^- \leq \theta \leq CI^+) = 1 - \alpha \quad (15)$$

Design-based approach defines this probability as an expected proportion of constructed confidence intervals, that under replicated sampling (from the same population and by identical sampling design) capture the true population value of a parameter  $\theta$ . A general requirement is that the true confidence level matches the nominal value  $1 - \alpha$ , where  $\alpha$  represents an expected proportion of intervals that do not hit the true population value. Reported 95% errors correspond to half-width of the above defined confidence intervals.

In section 2.7, we discussed the expected conservativeness of the URS approximate variance estimators of totals. We suppose that our confidence intervals of totals are conservative too, so the true confidence level likely exceeds the nominal value. Conservative confidence intervals are in fact somewhat safer than expected and somewhat wider than necessary.

### Prediction of crown age

DC specimens exhibit a peculiar growth pattern, which was described in detail by Adolt & Pavliš (2004). Under normal circumstances, first branching of the tree axes corresponding to the creation of crown is induced by first flowering of the tree's terminal node. Strictly speaking, the methodology of DC age estimation developed so far can be used to predict crown age only. Nonetheless, this partial information is useful because most DC specimens in Firmihin have already formed a crown. The principles of the methodology were formulated by Adolt & Pavliš (2004), who also made the first attempt to derive a statistical model for crown age prediction. Quite recently Adolt et al. (2012) parametrized a more suitable logistic regression model based on an extended data set from two different localities on Socotra - Firmihin and Skant. In the present study, all crown age predictions were obtained from this updated model using mean number of branching orders on peripheral branches as the only explanatory variable.

For each stem registered in the smaller circle ( $r = 15$  m) crown age was calculated in three variants. The first and most likely one corresponds to model fit. The remaining two used lower and upper limits of crown age predictions derived from the narrow (non-simultaneous) confidence band of the model. Table 9 and figure 6 in the appendix show DC crown age predictions as a function of mean number of branching orders.

## RESULTS

Area of accessible land was estimated to 648.66 ha, which is almost 95% of the total area of Firmihin AOI. Table 4 shows the resulting figures and their precision.

**Table 4: Estimated total area of accessible land.** Proportion of accessible land to the total area of Firmihin AOI (687.20 ha) is presented in the second row.

Parameter	Est. total/proportion	95% error	95% error (%)
area of accessible land [ha]	648.66	30.51	4.70
proportion of accessible land	0.9439	0.0444	4.70

The total was obtained by (8) using local density according to (6). Notice identical relative precisions of total and proportion of accessible land. This observation is logical as the proportion corresponds to  $\hat{Y}$  defined by (8).

Table 5 summarizes estimated DC stem counts, overall and partitioned by predicted crown age classes. Stem counts were calculated according to (8) substituting local densities defined by (7).

Stem densities per hectare of accessible land are found in table 6. They were estimated by (11). Total estimators defining the ratio were obtained by (8) using local densities (7) and (6) for the nominator and denominator.

**Table 5: Estimated total count of DC stems in Firmihin.** Crown age class up to 100 years includes also stems which have not formed any crown yet. Crown age prediction according to model fit, lower and upper bound are based on an earlier publication by Adolt et al. (2012).

parameter	Est. total	95% error	95% error (%)
Number of all stems (NOS)	66054	14500	22
NOS with a crown	65509	14360	22
NOS, crown age (CA) above 400 years	1999	951	48
NOS, CA between 100 and 200 years	18081	6001	33
NOS, CA between 200 and 300 years	24895	5609	23
NOS, CA between 300 and 400 years	12902	3000	23
NOS, CA up to 100 years	8177	4459	55
NOS, lower CA above 400 years	909	704	77
NOS, lower CA between 100 and 200 years	32618	8623	26
NOS, lower CA between 200 and 300 years	18808	4001	21
NOS, lower CA between 300 and 400 years	3453	1314	38
NOS, lower CA up to 100 years	10267	5224	51
NOS, upper CA above 400 years	15446	3264	21
NOS, upper CA between 100 and 200 years	6724	3167	47
NOS, upper CA between 200 and 300 years	21261	6403	30
NOS, upper CA between 300 and 400 years	19080	4314	23
NOS, upper CA up to 100 years	3543	2531	71

Age structure of the DC population in Firmihin is captured by shares of crown age classes on the overall number of living stems. The estimates (shown in table 7) were obtained using equation (11), in which necessary total estimators were calculated by (8). Local densities were defined according to (7) with  $C_i$  values adjusted to corresponding crown age classes (nominators specific for each crown age class) and  $C_i = 1 \forall i$  (constant denominator, an estimator of the total number of stems). A graphical representation of the estimated (crown) age structure of the DC population in Firmihin is shown in figure 5.

**Table 6: Estimated spatial densities of DC trees in Firmihin (stems per ha of accessible land).** Crown age class up to 100 years includes also stems which have not formed any crown yet. Crown age prediction according to model fit, lower and upper bound are based on an earlier publication by Adolt et al. (2012).

parameter	Est. density	95% error	95% error (%)
Density of all stems (DOS) [stems/ha]	102	22	22
DOS with a crown	101	22	21
DOS, crown age (CA) above 400 years	3	1	47
DOS, CA between 100 and 200 years	28	9	33
DOS, CA between 200 and 300 years	38	9	22
DOS, CA between 300 and 400 years	20	5	23
DOS, CA up to 100 years	13	7	54
DOS, lower CA above 400 years	1	1	78
DOS, lower CA between 100 and 200 years	50	13	26
DOS, lower CA between 200 and 300 years	29	6	21
DOS, lower CA between 300 and 400 years	5	2	38
DOS, lower CA up to 100 years	16	8	51
DOS, upper CA above 400 years	24	5	21
DOS, upper CA between 100 and 200 years	10	5	47
DOS, upper CA between 200 and 300 years	33	10	30
DOS, upper CA between 300 and 400 years	29	7	22
DOS, upper CA up to 100 years	5	4	71

**Table 7: Estimated age structure of DC population in Firmihin.** Shares of crown age classes refer to total number of stems (including stems without a crown). Crown age class up to 100 years includes also stems which have not formed any crown yet. Crown age prediction according to model fit, lower and upper bound are based on an earlier publication by Adolt et al. (2012).

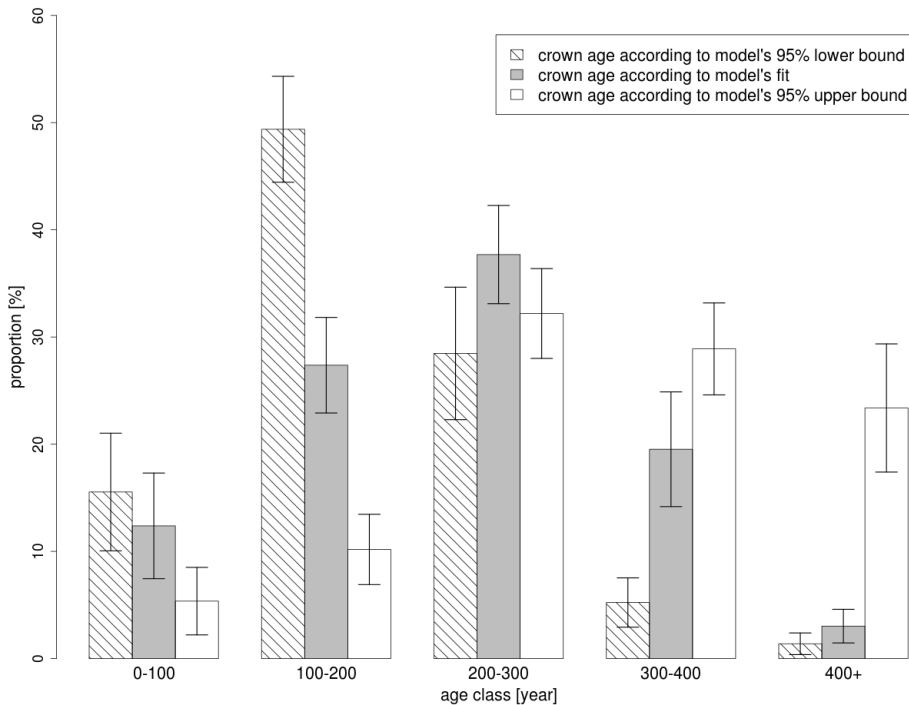
parameter	Est. share	95% error	95% error (%)
Share of stems (SOS), crown age above 400 years	0.0303	0.0157	51.98
SOS, crown age (CA) between 100 and 200 years	0.2737	0.0446	16.31
SOS, CA between 200 and 300 years	0.3769	0.0458	12.15
SOS, CA between 300 and 400 years	0.1953	0.0535	27.38
SOS, CA up to 100 years	0.1238	0.0493	39.84
SOS, lower CA above 400 years	0.0138	0.0101	73.48
SOS, lower CA between 100 and 200 years	0.4938	0.0494	9.99
SOS, lower CA between 200 and 300 years	0.2847	0.0618	21.71
SOS, lower CA between 300 and 400 years	0.0523	0.0230	44.05
SOS, lower CA up to 100 years	0.1554	0.0549	35.30
SOS, upper CA above 400 years	0.2338	0.0598	25.56
SOS, upper CA between 100 and 200 years	0.1018	0.0328	32.26
SOS, upper CA between 200 and 300 years	0.3219	0.0419	13.01
SOS, upper CA between 300 and 400 years	0.2889	0.0429	14.85
SOS, upper CA up to 100 years	0.0536	0.0315	58.70
SOS with a crown	0.9917	0.0073	0.73

Table 8 shows mean crown age of DC stems estimated as a ratio (11), where total estimators according to (8) correspond to total crown age (numerator) and total number of stems (denominator). Local density (7) used  $Y_i = A_i$  ( $A_i$  is the crown age predicted for stem  $i$ ) in the nominator and  $Y_i = 1 \forall i$  in the denominator of (11).

**Table 8: Mean crown age of DC population in Firmihin.** Crown age prediction according to model fit, lower and upper bound are based on an earlier publication by Adolt et al. (2012).

Parameter	Est.mean	95% error	95% error (%)
Crown age lower (year)	169.48	14.13	8.34
Crown age upper (year)	307.71	21.54	7.00
Crown age model fit (year)	226.16	17.31	7.65

**Fig. 5: Estimated age structure of DC population in Firmihin.** Shares of crown age classes refer to total number of stems (including stems without a crown). Crown age class up to 100 years includes also stems which have not formed any crown yet. Crown age prediction according to model fit, lower and upper bound are based on an earlier publication by Adolt et al. (2012). Vertical bars on the top of each column represent estimated 95% confidence intervals (uncertainty due to sampling).



## DISCUSSION

Relative accuracies summarized in tables 5, 6 and 7 are somewhat lower than might be expected by end-users. Largest relative errors, typically exceeding 50%, are observed for totals, spatial densities and shares of the first and last crown age class (up to 100 and over 400 years). DC specimens pertaining to any of these two crown age classes are relatively rare, so the corresponding local density is somewhat volatile over the Firmihin AOI. This problem was expected before the estimation has been run, therefore a moderate number of wider crown age classes was chosen. The wider the classes the better the accuracy, but at the same time, the less detail on crown age structure. Absolute 95% errors of all estimates seem acceptable, especially, when no comparable information exists.

In environmental surveys based on (quasi)systematic or spatially stratified sampling designs, URS variance estimators typically lead to overestimation of variance (see section 2.7). Results of many authors show that the overestimation might reach the order of 2 or even more provided the population features exhibit strong and positive spatial correlation (Cordy & Thompson 1995; Heikkinen, 2006). Overestimation of the confidence interval width and the 95% errors is still substantial, although it decreases with square root when switching from variance to these accuracy measures. Therefore, we expect that our results, especially total estimators based on original local densities, are in fact more accurate than reported. To approach the true level of accuracy several variance estimators were proposed (see references in section 2.7). We plan to use these elaborate estimators for our next publication.

Our current estimates involved only sample stems registered on smaller circular segments ( $r = 15$  m, full detail of stem attributes surveyed, see table 3). No additional information has been used during estimation except data collected in the field. In common terminology this approach can be characterized as one-phase, one-stage design (Mandallaz, 2007, section 4.2.).

For future publication we would like to use all available data collected in the field (including sample stems registered on larger circular segments with  $r = 25$  m) and also relevant auxiliary information which can be derived by remote sensing (classification of QuickBird or similar imagery). Working with digital QuickBird compositions during our field survey and based on results of a preliminary image classification, we concluded that QuickBird has enough potential to distinguish between areas covered by DC crowns and the other types of land-cover. Terrestrial data and the classified QuickBird imagery can be put together and estimates derived by means of two-phase sampling techniques (Mandallaz, 2007; section 5).

The above proposals might lead to moderate accuracy gains for the overall stem count, per hectare density of stems and the area shaded by DC crowns. Speaking about age structure, no significant increase of accuracy is expected because for stems located in the large circle no variables directly related to crown age were registered and this information can't be substituted by QuickBird imagery effectively. Quite often crowns of several trees are merged in to one image segment. Even if some crowns are correctly delineated, their size is not expected to correlate strongly with mean number of branching orders. Our earlier observations indicate that increasing age may be only partially reflected by crown size because the length of branch segments tends to decrease with age, so the age influences not only the size but also the inner structure and shape of crown (Adolt & Pavliš, 2004; figure 7).

Estimated age structure is captured in figure 5. The immediate and clear message here is that the population is overmature - an evident consequence of missing regeneration. In undisturbed, natural DC populations we would expect the highest relative abundance of the first few crown age classes and a strongly right-skewed shape of the distribution. A good

example can be seen in figure 6 (histogram for locality Scant) published by Adolt et al. (2012). In figure 5, only the histogram for lower crown age predictions (green columns) partially resembles a natural DC population. Overmaturity is obvious just by eye in many parts of Firmihin, so the indirect evidence presented here is rather redundant. It is also in agreement with conclusions of Habrová et al. (2009), who argues that DC populations on Socotra were threatened by overmaturity.

Let us compare the histogram for locality Firmihin according to Adolt et al. (2012; figure 7) with our actual results here (crown age according to the model fit). Of course, the model to predict crown age is the same, but the samples (plot positions and stems selected) are independent between the two surveys. Despite the independence of sampling, it is apparent that both histograms look pretty similar. Stems evaluated in the earlier publication were not selected by probability sampling, which was identified as one of the potential drawbacks. However, the observed concordance implies that also the former survey must be, at least to some degree, representative for the whole population in Firmihin. If it wasn't, crown age predictions could be biased for this particular reason.

It is also possible to compare the amount of uncertainty due to sampling with its amount related to crown age prediction (differences in proportions using model fit, lower and upper bounds). In figure 5, it is evident that the most uncertainty has to do with crown age prediction, not the sampling error. Hence, more accurate information on age structure can be obtained increasing prediction accuracy of the model rather than the current number or size of sample plots.

Adolt et al. (2012) proposed improvements in terms of data representativeness and an appropriate level of detail, on which measurements are taken. The authors suggest to register the presence-absence of flowers and fruits on the level of individual leaf rosettes. Representativeness is best achieved if data is collected using probability sampling. Plots established within the actual survey can serve this purpose. Furthermore, because the method of crown age prediction is based on observations of temporarily unstable variables - presence-absence of flowers and fruits, the survey must address also the time aspect of representativeness. In order to capture a seasonal variability of flowering a suitable inventory subgrid (a subset of the already established and surveyed sample plots) should be visited several times per year. Moreover, the survey should keep on running for several years to compensate for likely significant year to year variability of flowering.

Suggestions of Adolt et al. (2012) can be further extended by non-parametric model formulations, which could capture potential non-linear effects. Fahrmeir et al. (2013; section 9) provide a rich set of methods applicable to a variety of real-life modeling situations.

Mean crown age was estimated to 226 years with a confidence interval from 169 to 308 years depending on crown age prediction used - fit, lower or upper (neglecting the relatively low sampling error). This result seems biologically plausible although the model behind was formulated and parametrized using available rather than the most suitable data. This value is almost identical to simple arithmetic mean of predicted crown ages which was published by Adolt et al. (2012) (see the blue vertical line for Firmihin in figure 6).

Attorre et al. (2007) analyzed the current and potential distribution of DC over the Socotra Island. The authors concluded that the species currently occupies only 5.5% of its potential habitat and that the decline of DC population occurred in the past. They also hypothesized that the shrinkage of DC distribution was caused by human activities, soil-erosion, increased aridity and biotic interactions.

Let's have a look at the few DC specimens scattered over the plateaus adjacent to wadis Ezgeko and Darho. These trees are found in ecological conditions, which hardly differ from

those in Firmihin (historical accessibility being the only but likely decisive exception). Our guess is that these trees are remnants of former DC woodlands, the decline of which must have started long time ago. Therefore, the hypothesized past reduction of the DC distribution seems at least visually confirmed, perhaps not only in this particular area.

Our results suggest that DC populations in Firmihin and similar ecological conditions are fairly long-lived. Thus, the transition to overmaturity of the extent observed in Firmihin obviously started at least several decades ago (see figure 5). On the above mentioned plateaus the process of decline must have started even earlier, perhaps more than hundred years ago. Based on the above arguments we do not believe, that climate change was responsible for the apparently prolonged decline of DC regeneration.

We hypothesize that it is mainly pastoralism, the traditional source of livelihood for many generations of native people, which have been preventing DC populations from regeneration for such a long time. In our opinion there is no firm evidence suggesting that the other factors mentioned by Attorre et al. (2007) could contribute significantly to the almost 95% reduction of DC distribution.

The design and concept of our survey makes it possible to evaluate changes over time on stem by stem bases (plot center positions fixed by landmarks, individual DC stems digitally mapped) and to generalize this plot-level details to the whole DC population in Firmihin AOI. A repeated survey on identical plots and stems, five to ten years after the first survey, would certainly bring more insight into the DC population's dynamic. Mortality, regeneration and even the change of population's mean crown age can be evaluated on survivor stems and further generalized to the whole area. Informations from the repeated survey would be extremely useful to draw reliable conclusions about the future state of the DC population in Firmihin and to design and apply appropriate measures in order to preserve this ancient and worldwide unique ecosystem.

The presented methodology, borrowed from the field of national forest inventories, is fairly general, so it can be adjusted and applied to other localities, populations, species and even on the level of the whole Socotra Island.

## REFERENCES

- Adolt, R., & Pavliš, J. (2004). Age structure and growth of *Dracaena cinnabari* populations on Socotra. *Trees*, 18, pp. 43–53.
- Adolt, R., Habrová, H., & Maděra, P. (2012). Crown age estimation of a monocotyledonous tree species *Dracaena cinnabari* using logistic regression. *Trees*, 26, pp. 1287–1298.
- Attorre, F., Francesconi, F., Taleb, N., Scholte, P., Saed, A., Alfo, M., & Bruno, F. (2007). Will dragonblood survive the next period of climate change? Current and future potential distribution of *Dracaena cinnabari* (Socotra, Yemen). *Biological conservation*, 138(3-4), pp. 430–439.
- Axelrod, D.I. (1975). Evolution and biogeography of madrean-tethyan sclerophyll vegetation. In: Annals of the missouri botanical garden. *Missouri Botanical Garden Press*.
- Barabesi, L., & Franceschi, S. (2010). Sampling properties of spatial total estimators under tessellation stratified designs. *Environmetrics*, (on-line publication).
- Bellhouse, D., R. (1988). A brief history of random sampling methods. In: Krishnaiah, P., R., & Rao, C., R. (eds): *Handbook of statistics*, (pp. 1–13), sampling. 6, North Holland.
- Brown, G., & Mies, B.A. (2012). Vegetation ecology of Socotra. *Plant and Vegetation* 7., Springer, 382 pp.



- Buckland, S. T., Anderson, D. R., Burnham, K. P., & Laake, J. L. (1993). *Distance sampling: Estimating abundance of biological populations*. Chapman and Hall, London.
- Cassel, C.M., Särndal, C.E., & Wretman, J.H. (1977). *Foundations of inference in survey sampling*. John Wiley & Sons, New York. 192 p.
- Cochran, W. G. (1977). *Sampling techniques. Willey series in probability and mathematical statistics - applied*. John Wiley & Sons.
- Cooper, C.6. (2006). Sampling and variance estimation on continuous domains. *Environmetrics*, 17, pp. 539–553.
- Cordy, C., B., & Thompson, C., M. (1995). An application of the deterministic variogram to design-based variance estimation. *Mathematical geology*, 27, pp. 173–205.
- Cordy, C. B. (1993). An extension of the Horwitz-Thompson theorem to point sampling from a continuous universe. *Statistics and probability letters*, 18, pp. 353–362.
- De Sanctis, M., Adeeb, A., Farcomeni, A., Patriarca, Ch., A., Saed, & Attorre, F. (2013). Classification and distribution patterns of plant communities on Socotra Island, Yemen. *Applied vegetation science*, 16(1), pp. 148–165.
- Fahrmeir, L., Kneib, T., Lang, S., & Marx, B. (2013). *Regression*. Springer.
- Godambe, V.P. (1955). An unified theory of sampling from finite populations. *Journal of the Royal Statistical Society, series b*, 17, pp. 269–278.
- Gregoire, T. G., & Valentine, H. T. (2008). *Sampling strategies for natural resources and the environment*. Chapman and Hall/CRC.
- Haber, S. (1966). A modified Monte Carlo quadrature. *Math. comput.*, 20, pp. 361–368.
- Haber, S. (1967). A modified Monte Carlo quadrature 2. *Math. comput.*, 21, pp. 388–397.
- Habrová, H. (2004). Geobiocoenological differentiation as a tool for sustainable land-use of Socotra Island. *Ekologia*, 23, pp. 47–57.
- Habrová, H., & Maděra, P. (2004). Ecology of *Dracaena cinnabari* communities on Socotra. In: Polehla, P. (ed): *Geobiocoenological papers*, (pp. 120–126), vol. 9. MUAF in Brno.
- Habrová, H., Čermák, Z., & Pavliš, J. (2009). Dragon's blood tree - threatened by overmaturity, not by extinction: Dynamics of a *Dracaena cinnabari* woodland in the mountains of Socotra. *Biological conservation*, 142(4), pp. 772–778.
- Heikkinen, J. (eds. Kangas A. & Maltamo M.). (2006). *Forest inventory, methodology and applications*. Springer Verlag. Chap. Assessment of Uncertainty in Spatially Systematic Sampling, pp. 155–176.
- Hubálková, I. (2011). Prediction of dragon's blood tree (*Dracaena cinnabari* Balf.) stand sample density on Socotra Island (key study). *Journal of Landscape Ecology*, 4(2), pp. 5–20.
- Kangas, A., Gove, J. H., & Scott, T. Ch. (eds. Kangas A. & Maltamo M.). (2006). *Forest inventory, methodology and applications*. Springer Verlag. Chap. Introduction, pp. 3–8.
- Král, K., & Pavliš, J. (2006). The first detailed land cover map of Socotra Island by Landsat/ETM+ data. *International Journal of Remote Sensing*, 27(15), pp. 3239–3250.
- Kürschner, H., Hein, P., Kilian, N., & Hubaishan, M.A. (2006). Diversity and Zonation of the forests and woodlands of the Mountains of Northern Socotra, Yemen. *Englera*, 28, pp. 11–55.
- Laplace, P.S. (1783). Sur les naissances, les mariages et les morts. In: *Histoire de l'académie royale des sciences*, année 1783. Académie Royale des Sciences, Paris.

- Mandallaz, D. (1991). *An unified approach to sampling theory for forest inventory based on infinite population and superpopulation models*. Ph.D. thesis, Swiss-Federal Institute of Technology (ETH), Zurich.
- Mandallaz, D. (2007). *Sampling techniques for forest inventories*. Chapman and Hall/CRC.
- Marrero, A., Almeida, S.R., & Martín-González, M. (1998). A new species of the wild dragon tree, *Dracaena* (Dracaenaceae) from Gran Canaria and its taxonomic and biogeographic implications. *Botanical Journal of the Linnean Society*, 128(3), pp. 291–314.
- Matérn, B. (1960). *Spatial variation*. Ph.D. thesis, Statens Skogsforskningsinstitut.
- Mies, B., & Beyhl, F.E. (1996). The vegetation Ecology of Soqotra. In: Dumont, H.J. (ed): *Proceedings of the first International Symposium on Soqotra Island*, (pp. 35–82). Aden, NY. United Nations Publications.
- Miller, A., & Cope, T.A. (1996). *Flora of the Arabian Peninsula and Socotra*. Vol. 1., Edinburgh University Press.
- Miller, A., & Morris, M. (eds). (2000). *Conservation and sustainable use of the biodiversity of soqotra archipelago*. Royal Botanic Garden Edinburgh.
- Miller, A.G., Morris, M., Diccon, A., & Atkinson, R. (2004). *Ethnoflora of the Soqotra Archipelago*. Royal Botanic Garden Edinburgh.
- Neyman, J. (1934). On the two different aspects of the representative sampling: the method of stratified sampling and the method of purposive sampling. *Journal of the Royal Statistical Society*, pp. 558–606.
- Quenouille, M. H. (1949). Problems in plane sampling. *Annals of Mathematical Statistic*, 20, pp. 335–375.
- R Core Team. (2013). *R: A language and environment for statistical computing*. R Foundation for Statistical Computing, Vienna, Austria.
- Rao, J. N. K. (2003). *Small area estimation*. Wiley.
- Razdorskij, F., V. (1954). *Anatomie rostlin*. ČSAV. Praha.
- Ripley, B. D. (2004). *Spatial statistics*. John Wiley & Sons.
- Scholte, P., & De Geest, P. (2010). The Climate of Socotra Island (Yemen): A first-time assessment of the timing of the monsoon wind reversal and its influence on precipitation and vegetation patterns. *Journal of Arid Environments*, 74, pp. 1507–1515.
- Scholte, P., Al-Okaishi, A., & Suleyman, A.S. (2011). When conservation precedes development: A case study of the opening up of the Socotra Archipelago, Yemen. *Oryx*, 45(3), pp. 401–410.
- Stevens, D. L. Jr. (1997). Variable density grid-based sampling designs for continuous spatial populations. *Environmetrics*, 8, pp. 167–195.
- Stevens, D. L. Jr., & Olsen, A. R. (2003). Variance estimation for spatially balanced samples of environmental resources. *Environmetrics*, 14, pp. 593–610.
- Stevens, D. L. Jr., & Olsen, A. R. (2004). Spatially balanced sampling of natural resources. *Journal of the American Statistical Association*, 99, pp. 262–278.
- Särndal, C. E., Swensson, B., & Wretman, J. (2003). *Model assisted survey sampling*. Springer.
- Van Damme, K., & Banfield, L. (2011). *Past and present human impacts on the biodiversity of Socotra Island (Yemen): implications for future conservation*. *biodiversity conservation in the Arabian Peninsula zoology in the Middle East*, Heidelberg: Kasperek Verlag.

Supplementum 3: pp. 31–88.

Zimmermann, M., H., & Tomlinson, P., B. (1969). The vascular system in the axis of *Dracaena fragrans* (Agavacea). *Journal of the Arnold Arboretum*, 50, pp. 370–383.

## APPENDIX

**Fig. 6: Crown age predictions for *D. cinnabari* and their confidence bands.** Predictions are based on a mean number of branching orders observed on crown periphery (Adolt et al., 2012).

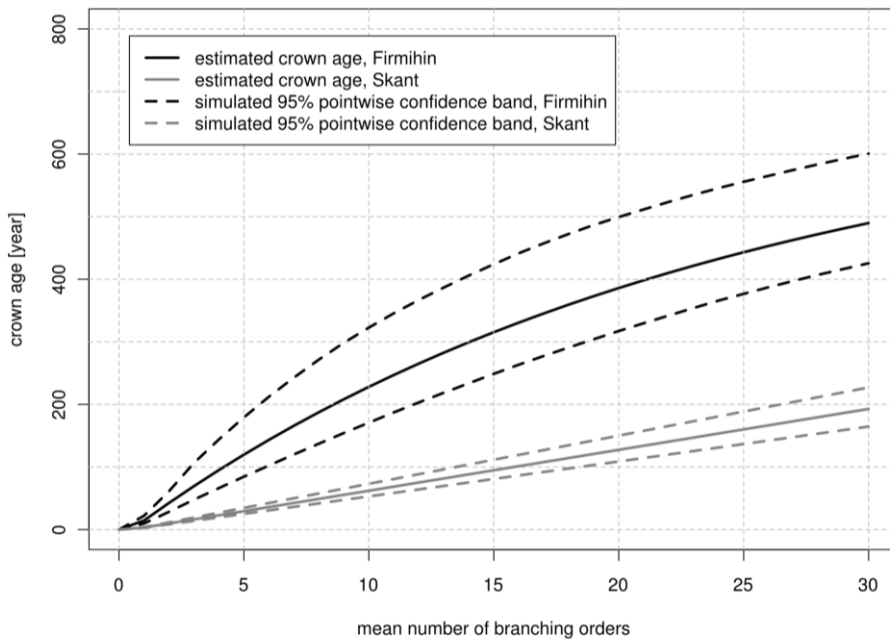


**Table 9: Crown age predictions for *D. cinnabari* and related confidence intervals.**

The term  $X_1$  stands for mean number of branching orders (Adolt et al., 2012).

model	firmihin.03q			skant.03q		
locality	Firmihin			Skant		
$X_1$	fit	lower	upper	fit	lower	upper
1	14	10	22	3	3	4
2	41	28	61	10	8	12
3	70	48	106	16	14	19
4	97	66	144	23	20	27
5	122	84	179	29	25	35
6	146	102	212	36	31	42
7	169	120	243	42	36	50
8	191	137	272	49	42	58
9	212	154	298	56	47	65
10	233	171	322	62	53	73
11	252	187	346	69	59	81
12	271	203	367	75	64	88
13	288	219	387	82	70	96
14	305	234	406	88	75	104
15	322	249	424	95	81	112
16	337	264	442	101	86	119
17	352	277	457	108	92	127
18	367	291	472	114	98	135
19	381	304	487	121	103	142
20	394	317	499	127	109	150
21	406	330	512	134	114	158
22	419	342	524	140	120	166
23	430	354	535	147	126	173
24	442	366	546	154	131	181
25	452	377	556	160	137	189
26	462	387	565	167	142	196
27	472	397	575	173	148	204
28	482	407	584	180	154	212
29	491	416	592	186	159	219
30	500	426	601	193	165	227